Population densities of hydrogenlike ions in a non-Maxwellian plasma

J. M. A. Ashbourn*
Clare Hall, University of Cambridge, Cambridge CB3 9AL, England
(Received 24 July 2000; published 29 March 2001)

In this paper we examine the effects of non-Maxwellian electron energy distributions on the population densities of excited atomic levels for hydrogenlike ions. We model the electron energy distribution function by two Maxwellian finite elements, one approximating the bulk distribution with temperature T_b and the other the tail distribution with temperature T_t. We present results for various T_b/T_t ratios for Si XIV.

DOI: 10.1103/PhysRevE.63.047402 PACS number(s): 52.20.Hv, 52.25.Os, 52.20.Fs

I. INTRODUCTION

Many astrophysical and laboratory plasmas have been found to have non-Maxwellian electron distributions, e.g., solar plasmas [1,2] and many laser-produced plasmas [3]. It is therefore of interest to study the influence that the high energy tail of the electron energy distribution function has on the population densities of various ions in such plasmas.

In this paper, we consider non-Maxwellian electron distributions which can be described by two finite Maxwellian elements at two different temperatures, one being the bulk electron temperature T_b, and the other being the tail electron temperature T_t for the tail of the distribution function. The first represents the distribution in the energy region $0 \leqslant E \leqslant E_c$ and the second that in the energy region $E_c \leqslant E \leqslant \infty$ (when $T_t > T_b$), where E_c is the joining point of the two regions. At $E = E_c$ the distribution is continuous. We have modified the collisional-radiative program COLRAD [4] to include the effect of having two differing temperatures in different energy regions. We consider the tail temperature to only affect transitions from the $n=1$ level to all other levels (i.e., only electron impact excitation and ionization from the ground state) and the bulk temperature to affect all other transitions from levels i to j, where $i \neq 1$.

II. CALCULATION OF NON-MAXWELLIAN POPULATION DENSITIES

The program COLRAD uses a collisional-radiative model, and the processes which are affected by the tail temperature are all electron collision transitions from the ground state, $1S_{1/2}$, to any other allowed level:

(i) Excitation by electron impact from the ground state,

$$\mathrm{H}(1S_{1/2}) + e \rightarrow \mathrm{H}(j) + e.$$

(ii) Ionization by electron impact from the ground state,

$$\mathrm{H}(1S_{1/2}) + e \rightarrow \mathrm{H}^+ + 2e.$$

Here j labels the atomic levels. All other processes involve only the bulk temperature for the calculation of the rate coefficients for each process. The rate coefficients for the inverse transitions down to the ground state from all allowed levels are normally calculated by the principle of detailed balance from the rate coefficients for the original transitions from $1S_{1/2}$ to these levels [4]—the latter are calculated as described in Refs. [5,6] for excitation, and as in Ref. [7] for ionization. Since, however, the rate coefficients for the inverse processes depend on the bulk temperature, and not the tail temperature (which is used for the original rate coefficients for transitions from the ground state), in order to obtain these the calculations need to be repeated using the bulk temperature T_b before applying detailed balance.

Results for hydrogenlike Si XIV

In this paper, we present the results for calculations of the population densities of the fine structure levels $1S_{1/2}$ to $3D_{5/2}$, using COLRAD, for the hydrogenlike ion Si XIV, present as a small admixture in a hydrogen base plasma; we consider silicon since it is an element of interest in studies of both astrophysical and laboratory plasmas. The bulk electron temperatures considered, T_b, are 250 and 500 eV, while the tail electron temperature, T_t, for the non-Maxwellian distribution function is varied around each of these bulk temperatures by increasing it by a factor of 2 and then decreasing it by a factor of $\frac{1}{2}$ for each value of T_b. The ion temperature is set equal to the bulk electron temperature for the cases considered below. We assume that E_c is less than the first inelastic threshold $|E(1S_{1/2}) - E(2P_{1/2})|$.

Tables I and II show the results for the excited level population densities against the electron density for various bulk and tail temperatures considered as described above, and it can be seen that using a non-Maxwellian distribution varies the population densities of each fine structure level quite markedly from their Maxwellian values. If the tail temperature is twice as large as the bulk electron temperature with $T_b = 250\,\mathrm{eV}$, it can be seen from Table I that the non-Maxwellian population density is decreased from the Maxwellian population density value by over two orders of magnitude for the ground state, $1S_{1/2}$, and is decreased by up to an order of magnitude for all other excited levels. When the tail temperature is half the bulk temperature, the non-Maxwellian population density for the $1S_{1/2}$ level is seen to be increased by over two orders of magnitude from the Maxwellian value, but this time the other excited levels are decreased by over an order of magnitude (sometimes nearly two orders) from the Maxwellian population density values, which is a much greater reduction in magnitude than that

*Email address: J.M.A.Ashbourn@damtp.cam.ac.uk

TABLE I. Table of population densities for the fine structure levels $1S_{1/2}$ to $3D_{5/2}$ against n_e for Si XIV in a hydrogen base plasma with $T_b = 250$ eV and $T_t = 250$ eV (Maxwellian), 500 eV (non-Maxwellian), and 125 eV (non-Maxwellian).

Level \ n_e (cm^{-3})	10^{14}	10^{15}	10^{16}	10^{17}	10^{18}	10^{19}	10^{20}
			$T_t = 250$ eV (Maxwellian)				
$1S_{1/2}$	3.041×10^{18}	3.000×10^{19}	2.929×10^{20}	2.806×10^{21}	2.603×10^{22}	2.295×10^{23}	1.864×10^{24}
$2S_{1/2}$	1.347×10^{10}	6.533×10^{11}	1.048×10^{13}	1.075×10^{14}	1.013×10^{15}	9.470×10^{15}	1.205×10^{17}
$2P_{1/2}$	5.861×10^{4}	7.167×10^{6}	8.085×10^{8}	7.921×10^{10}	7.349×10^{12}	6.481×10^{14}	5.200×10^{16}
$2P_{3/2}$	1.110×10^{5}	1.132×10^{7}	1.133×10^{9}	1.088×10^{11}	1.005×10^{13}	8.889×10^{14}	7.337×10^{16}
$3S_{1/2}$	1.956×10^{5}	1.932×10^{7}	1.854×10^{9}	1.483×10^{11}	5.610×10^{12}	1.413×10^{14}	6.205×10^{15}
$3P_{1/2}$	8.928×10^{3}	8.828×10^{5}	8.705×10^{7}	9.027×10^{9}	1.033×10^{12}	9.239×10^{13}	5.939×10^{15}
$3P_{3/2}$	1.785×10^{4}	1.764×10^{6}	1.722×10^{8}	1.656×10^{10}	1.573×10^{12}	1.331×10^{14}	1.018×10^{16}
$3D_{3/2}$	6.748×10^{3}	6.709×10^{5}	6.589×10^{7}	6.361×10^{9}	6.446×10^{11}	8.469×10^{13}	9.559×10^{15}
$3D_{5/2}$	1.012×10^{4}	1.006×10^{6}	9.880×10^{7}	9.516×10^{9}	9.399×10^{11}	1.132×10^{14}	1.332×10^{16}
			$T_t = 500$ eV (non-Maxwellian)				
$1S_{1/2}$	1.149×10^{16}	1.146×10^{17}	1.142×10^{18}	1.134×10^{19}	1.121×10^{20}	1.101×10^{21}	1.081×10^{22}
$2S_{1/2}$	2.129×10^{9}	1.044×10^{11}	1.710×10^{12}	1.821×10^{13}	1.833×10^{14}	1.911×10^{15}	2.959×10^{16}
$2P_{1/2}$	9.615×10^{3}	1.180×10^{6}	1.353×10^{8}	1.371×10^{10}	1.353×10^{12}	1.332×10^{14}	1.296×10^{16}
$2P_{3/2}$	1.825×10^{4}	1.879×10^{6}	1.917×10^{8}	1.903×10^{10}	1.864×10^{12}	1.841×10^{14}	1.846×10^{16}
$3S_{1/2}$	6.481×10^{4}	6.464×10^{6}	6.321×10^{8}	5.247×10^{10}	2.117×10^{12}	5.998×10^{13}	3.279×10^{15}
$3P_{1/2}$	3.009×10^{3}	3.007×10^{5}	3.022×10^{7}	3.236×10^{9}	3.934×10^{11}	3.940×10^{13}	3.140×10^{15}
$3P_{3/2}$	6.018×10^{3}	6.008×10^{5}	5.980×10^{7}	5.945×10^{9}	6.015×10^{11}	5.748×10^{13}	5.448×10^{15}
$3D_{3/2}$	2.775×10^{3}	2.777×10^{5}	2.773×10^{7}	2.771×10^{9}	2.932×10^{11}	3.985×10^{13}	5.195×10^{15}
$3D_{5/2}$	4.162×10^{3}	4.165×10^{5}	4.159×10^{7}	4.147×10^{9}	4.298×10^{11}	5.424×10^{13}	7.311×10^{15}
			$T_t = 125$ eV (non-Maxwellian)				
$1S_{1/2}$	4.948×10^{20}	5.003×10^{21}	5.107×10^{22}	5.305×10^{23}	5.684×10^{24}	6.431×10^{25}	8.035×10^{26}
$2S_{1/2}$	1.055×10^{9}	5.241×10^{10}	8.791×10^{11}	9.770×10^{12}	1.062×10^{14}	1.275×10^{15}	2.481×10^{16}
$2P_{1/2}$	4.474×10^{3}	5.634×10^{5}	6.665×10^{7}	7.086×10^{9}	7.599×10^{11}	8.582×10^{13}	1.056×10^{16}
$2P_{3/2}$	8.462×10^{3}	8.850×10^{5}	9.275×10^{7}	9.668×10^{9}	1.034×10^{12}	1.170×10^{14}	1.478×10^{16}
$3S_{1/2}$	7.931×10^{3}	8.043×10^{5}	8.074×10^{7}	6.988×10^{9}	3.014×10^{11}	9.568×10^{12}	7.914×10^{14}
$3P_{1/2}$	3.063×10^{2}	3.109×10^{4}	3.215×10^{6}	3.656×10^{8}	4.997×10^{10}	6.032×10^{12}	7.517×10^{14}
$6P_{3/2}$	6.124×10^{2}	6.210×10^{4}	6.348×10^{6}	6.616×10^{8}	7.418×10^{10}	9.119×10^{12}	1.398×10^{15}
$3D_{3/2}$	7.476×10^{2}	7.646×10^{4}	7.925×10^{6}	8.402×10^{8}	9.223×10^{10}	1.065×10^{13}	1.483×10^{15}
$3D_{5/2}$	1.121×10^{3}	1.147×10^{5}	1.189×10^{7}	1.260×10^{9}	1.380×10^{11}	1.571×10^{13}	2.203×10^{15}

observed for these levels when the tail temperature is twice the bulk temperature.

For a bulk electron temperature (and hence ion temperature) of 500 eV, it can be seen from Table II that for $T_t = 2T_b$ the magnitude of the reduction in the population densities for all the levels is smaller than that in Table I. In all cases, the population density for the ground state is reduced by over an order of magnitude from the Maxwellian value, while the remaining levels are reduced by about a factor of 3 from their Maxwellian values. For $T_t = \frac{1}{2}T_b$, the population density for the ground state is increased by over two orders of magnitude this time, and those for the other excited levels are increased by about a factor of 3, although this decreases in magnitude for the higher n excited levels.

Figures 1–3 show graphs of the population densities of the $1S_{1/2}$, $2P_{1/2}$, and $3P_{1/2}$ levels, respectively, against electron density n_e, for the case when $T_b = 250$ eV, with T_t having both a Maxwellian value and the two non-Maxwellian values produced by varying it around T_b by factors of 2 and $\frac{1}{2}$, as described previously. The graphs show how the population densities for these selected levels vary with the value of the tail electron temperature and that this effect is nearly independent of the electron density.

III. CONCLUSION AND DISCUSSION

It can be seen from Tables I and II and Figs. 1–3 that having a non-Maxwellian electron distribution very significantly varies the population density of each level from its Maxwellian value. This effect seems to be at a maximum for the case when the bulk electron temperature has the lowest value considered here, 250 eV. Figures 1–3 show a nearly linear relationship between the population densities and the electron density—this is because from the collisional-radiative model the rate of change of population density for a particular level [4] varies linearly with the electron density in all terms for the collisional processes involved—apart from that for the three-body recombination process, which varies as the square of the electron density; thus the three-body recombination rate is only important at higher plasma densi-

TABLE II. As in Table I, but with $T_e = 500$ eV, and $T_e = 500$ eV (Maxwellian), 1 keV (non-Maxwellian), and 250 eV (non-Maxwellian).

Level \ n_e (cm^{-3})	10^{14}	10^{15}	10^{16}	10^{17}	10^{18}	10^{19}	10^{20}
			$T_t = 500$ eV (Maxwellian)				
$1S_{1/2}$	6.765×10^{15}	6.711×10^{16}	6.612×10^{17}	6.434×10^{18}	6.119×10^{19}	5.591×10^{20}	4.756×10^{21}
$2S_{1/2}$	1.259×10^{9}	6.192×10^{10}	1.010×10^{12}	1.056×10^{13}	1.023×10^{14}	9.882×10^{14}	1.302×10^{16}
$2P_{1/2}$	5.627×10^{3}	6.791×10^{5}	7.665×10^{7}	7.608×10^{9}	7.217×10^{11}	6.605×10^{13}	5.565×10^{15}
$2P_{3/2}$	1.074×10^{4}	1.107×10^{6}	1.124×10^{8}	1.094×10^{10}	1.031×10^{12}	9.463×10^{13}	8.214×10^{15}
$3S_{1/2}$	3.834×10^{4}	3.805×10^{6}	3.687×10^{8}	3.025×10^{10}	1.195×10^{12}	3.050×10^{13}	1.389×10^{15}
$3P_{1/2}$	1.766×10^{3}	1.755×10^{5}	1.743×10^{7}	1.814×10^{9}	2.096×10^{11}	1.942×10^{13}	1.324×10^{15}
$3P_{3/2}$	3.532×10^{3}	3.507×10^{5}	3.455×10^{7}	3.375×10^{9}	3.314×10^{11}	2.943×10^{13}	2.335×10^{15}
$3D_{3/2}$	1.562×10^{3}	1.556×10^{5}	1.537×10^{7}	1.497×10^{9}	1.513×10^{11}	1.927×10^{13}	2.184×10^{15}
$3D_{5/2}$	2.344×10^{3}	2.334×10^{5}	2.305×10^{7}	2.243×10^{9}	2.229×10^{11}	2.660×10^{13}	3.089×10^{15}
			$T_t = 1$ keV (non-Maxwellian)				
$1S_{1/2}$	3.755×10^{14}	3.745×10^{15}	3.727×10^{16}	3.693×10^{17}	3.631×10^{18}	3.522×10^{19}	3.331×10^{20}
$2S_{1/2}$	4.135×10^{8}	2.046×10^{10}	3.372×10^{11}	3.593×10^{12}	3.609×10^{13}	3.705×10^{14}	5.495×10^{15}
$2P_{1/2}$	1.952×10^{3}	2.347×10^{5}	2.660×10^{7}	2.683×10^{9}	2.626×10^{11}	2.554×10^{13}	2.398×10^{15}
$2P_{3/2}$	3.737×10^{3}	3.865×10^{5}	3.954×10^{7}	3.912×10^{9}	3.797×10^{11}	3.700×10^{13}	3.583×10^{15}
$3S_{1/2}$	1.822×10^{4}	1.816×10^{6}	1.777×10^{8}	1.485×10^{10}	6.081×10^{11}	1.665×10^{13}	8.682×10^{14}
$3P_{1/2}$	8.594×10^{2}	8.583×10^{4}	8.603×10^{6}	9.090×10^{8}	1.082×10^{11}	1.068×10^{13}	8.283×10^{14}
$3P_{3/2}$	1.719×10^{3}	1.715×10^{5}	1.706×10^{7}	1.694×10^{9}	1.719×10^{11}	1.636×10^{13}	1.476×10^{15}
$3D_{3/2}$	8.884×10^{2}	8.882×10^{4}	8.852×10^{6}	8.786×10^{8}	9.056×10^{10}	1.153×10^{13}	1.400×10^{15}
$3D_{5/2}$	1.333×10^{3}	1.332×10^{5}	1.327×10^{7}	1.316×10^{9}	1.338×10^{11}	1.609×10^{13}	1.993×10^{15}
			$T_t = 250$ eV (non-Maxwellian)				
$1S_{1/2}$	9.504×10^{17}	9.421×10^{18}	9.421×10^{18}	9.029×10^{20}	8.560×10^{21}	7.688×10^{22}	6.099×10^{23}
$2S_{1/2}$	4.238×10^{9}	2.083×10^{11}	2.083×10^{11}	3.544×10^{13}	3.413×10^{14}	3.241×10^{15}	3.958×10^{16}
$2P_{1/2}$	1.828×10^{4}	2.219×10^{6}	2.219×10^{6}	2.500×10^{10}	2.370×10^{12}	2.129×10^{14}	1.667×10^{16}
$2P_{3/2}$	3.485×10^{4}	3.595×10^{6}	3.595×10^{6}	3.566×10^{10}	3.367×10^{12}	3.032×10^{14}	2.442×10^{16}
$3S_{1/2}$	6.263×10^{4}	6.225×10^{6}	6.225×10^{6}	4.950×10^{10}	1.947×10^{12}	4.848×10^{13}	2.036×10^{15}
$3P_{1/2}$	2.829×10^{3}	2.812×10^{5}	2.812×10^{5}	2.921×10^{9}	3.377×10^{11}	3.069×10^{13}	1.939×10^{15}
$3P_{3/2}$	5.657×10^{3}	5.620×10^{5}	5.620×10^{5}	5.429×10^{9}	5.320×10^{11}	4.619×10^{13}	3.405×10^{15}
$3D_{3/2}$	2.221×10^{3}	2.228×10^{5}	2.228×10^{5}	2.169×10^{9}	2.216×10^{11}	2.888×10^{13}	3.166×10^{15}
$3D_{5/2}$	3.331×10^{3}	3.343×10^{5}	3.343×10^{5}	3.247×10^{9}	3.206×10^{11}	3.961×10^{13}	4.466×10^{15}

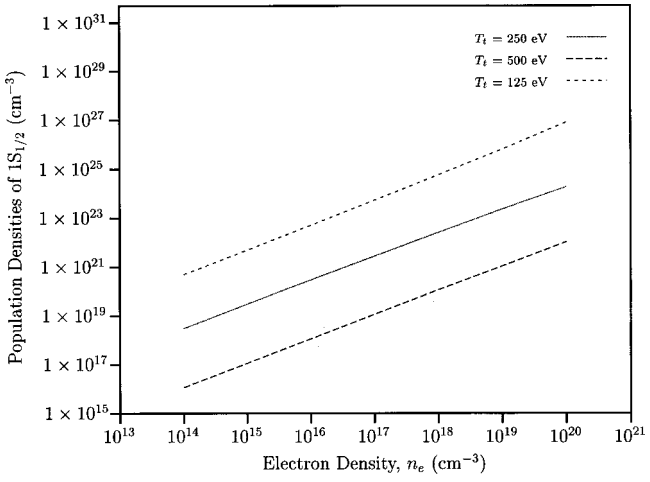

FIG. 1. A graph of the population densities for the $1S_{1/2}$ level against n_e for Si XIV in a hydrogen base plasma, with $T_b = 250$ eV and $T_t = 125$, 250 (Maxwellian), and 500 eV.

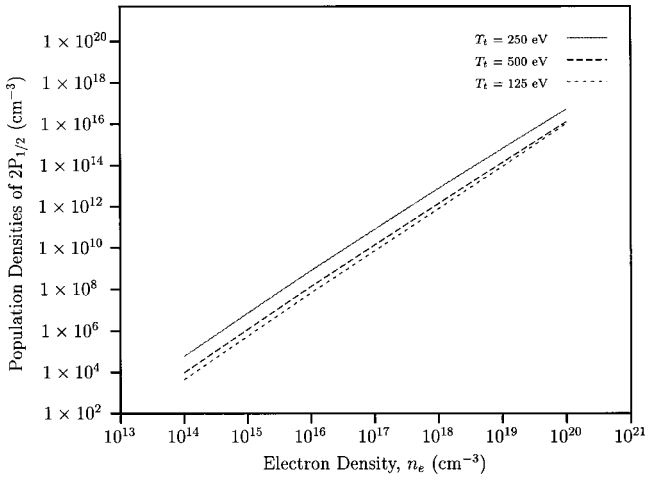

FIG. 2. A graph of the population densities for the $2P_{1/2}$ level against n_e for Si XIV in a hydrogen base plasma, with $T_b = 250$ eV and $T_t = 125$, 250 (Maxwellian), and 500 eV.

ties and is also preferentially stronger into upper levels than into the lower ones (such as the ground state) considered here.

When T_t is greater than T_b, the populations of all excited levels are decreased from their Maxwellian values as a result of the rates of depopulation of those levels having increased over the rates of population. Since T_t is considered to only affect transitions from the ground state to all other levels, this means that the rates of electron ionization and electron impact excitation from the ground state are increased from those for the Maxwellian case, which has a knock-on effect on the higher levels considered in our analysis. The rates of radiative decay are therefore unaffected by T_t, which means that the electron ionization and electron impact excitation processes dominate over radiative decay in the non-Maxwellian situation where $T_t > T_b$.

When T_t is smaller than T_b, the ground state population is increased from its Maxwellian value, since radiative decay down to the ground state dominates as a population mechanism over depopulation of the level by electron ionization and electron impact excitation when $T_t < T_b$. Since the ground state is being populated faster than it is being depopulated, this means that the rate of population of the higher levels from the ground state will be smaller, and hence that the higher excited level populations will be decreased.

As the overall bulk electron temperature considered is increased (as in Table II, from the value in Table I), the effect observed on the ground state is as described above, but of smaller magnitude than observed in Table I; the other excited level populations are decreased when $T_t > T_b$ and are increased when $T_t < T_b$.

A more detailed explanation of these effects requires a further analysis of the cross sections with the two temperatures considered. The results presented here from our implementation of non-Maxwellian electron distributions in COLRAD, for a high-temperature plasma, can reduce the differences previously noted (e.g., Refs. [8], [9]) between experimental and theoretical populations, and hence Lyman-α intensity ratios (when Maxwellian distributions were assumed), as non-Maxwellian distributions can often occur in both tokamaks and laser-produced plasmas.

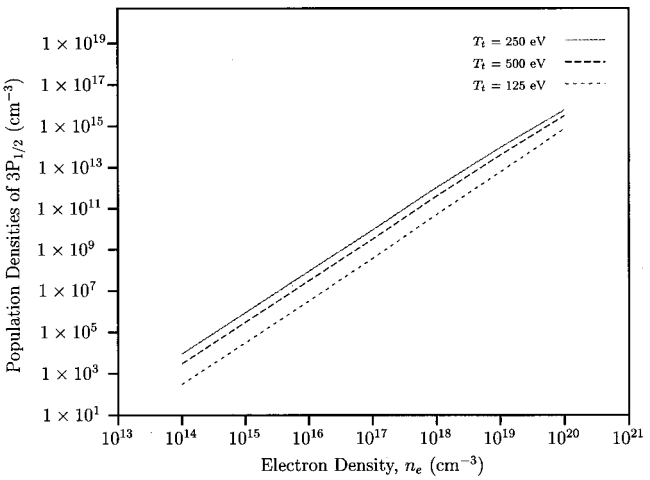

FIG. 3. A graph of the population densities for the $3P_{1/2}$ level against n_e for Si XIV in a hydrogen base plasma, with $T_b = 250$ eV and $T_t = 125$, 250 (Maxwellian), and 500 eV.

ACKNOWLEDGMENTS

The author would like to thank Dr. N. N. Ljepojević for useful discussions. Part of this work was completed under a research scholarship from the Center for Computer and Mathematical Modelling, South Bank University, London.

[1] A. G. Emslie, Sol. Phys. **86**, 133 (1983).

[2] R. Roussel-Dupre, Sol. Phys. **68**, 243 (1980).

[3] W. L. Kruer, *The Physics of Laser Plasma Interactions* (Addison-Wesley, Redwood City, CA, 1988).

[4] N. N. Ljepojević, R. J. Hutcheon, and J. Payne, Comput. Phys. Commun. **44**, 157 (1987).

[5] R. E. H. Clark, D. H. Sampson, and S. T. Goett, Astrophys. J., Suppl. **49**, 545 (1982).

[6] L. B. Golden and D. H. Sampson, Astrophys. J. **170**, 181 (1971).

[7] D. H. Sampson and L. B. Golden, J. Phys. B **11**, 541 (1978).

[8] H. Kubo, A. Sakasai, Y. Koide, and T. Sugie, Phys. Rev. A **46**, 7877 (1992).

[9] R. Bartiromo, F. Bombarda, and R. Giannella, Phys. Rev. A **40**, 7387 (1989).